Maps of the Cosmos
ASP Conference Series, Vol. 216, 2005
M. Colless, L. Staveley-Smith, R. Stathakis

Imaging the Cosmic Microwave Background with the Arcminute Cosmology Bolometer Array Receiver

J. B. Peterson,[1] A. K. Romer,[1] P. L. Gomez,[1] P. A. R. Ade,[2] J. J. Bock,[3] J. R. Bond,[4] C. R. Contaldi,[4] D. Pogosyan,[4] C. Cantalupo,[5] M. D. Daub,[6] W. L. Holzapfel,[6] M. Lueker,[6] M. Newcomb,[6] D. Woolsey,[6] C. L. Kuo,6,[7] A. E. Lange,[7] M. C. Runyan,[7,8] J. Ruhl,[9] J. H. Goldstein,[9,10] and E. Torbet[10]

[1]*Department of Physics, Carnegie Mellon University, Pittsburgh, PA 15213*
[2]*Department of Physics and Astronomy, Cardiff University, CF24 3YB Wales, UK*
[3]*Jet Propulsion Laboratory, Pasadena, CA 91125*
[4]*Canadian Institute for Theoretical Astrophysics, University of Toronto, Canada*
[5]*Lawrence Berkeley National Laboratory, Berkeley, CA 94720*
[6]*Department of Physics, University of California at Berkeley, Berkeley, CA 94720*
[7]*Department of Physics, Math, and Astronomy, California Institute of Technology, Pasadena, CA 91125*
[8]*Department of Physics, University of Chicago, Chicago, IL 60637*
[9]*Department of Physics, Case Western Reserve University, Cleveland, OH 44106*
[10]*Department of Physics, University of California, Santa Barbara, CA 93106*

Abstract. The Arcminute Cosmology Bolometer Array Receiver (ACBAR) is a multifrequency millimeter-wave receiver optimized for observations of the Cosmic Microwave Background (CMB) and the Sunyaev-Zel'dovich (SZ) effect in clusters of galaxies. ACBAR was installed on the 2.1 m Viper telescope at the South Pole in January 2001 and the results presented here incorporate data through July 2002. The power spectrum of the CMB at 150 GHz over the range $\ell = 150 - -3000$ measured by ACBAR is presented along with estimates for the values of the cosmological parameters within the context of ΛCDM models. The inclusion of Ω_Λ greatly improves the fit to the power spectrum. Three-frequency images of the SZ decrement/increment are also presented for the galaxy cluster 1E0657−67.

1. Instrument and Telescope

The Arcminute Cosmology Bolometer Array Receiver (ACBAR), a 16 pixel, millimeter wavelength, 240 mK bolometer array, is described in detail in Runyan et al. (2003). The instrument was designed to couple to the existing Viper tele-

scope at the South Pole to produce high resolution maps of the CMB sky with high signal-to-noise.

ACBAR is used to observe simultaneously at 150, 220, and 275 GHz with bandwidths of 31, 31 and 48 GHz, respectively. ACBAR makes use of extremely sensitive microlithographed spider-web bolometers developed at JPL for the Planck satellite mission (Turner et al. 2001). These detectors achieve background photon limited performance in ACBAR. In 2002 the 150 GHz channels had an average NET_{RJ} sensitivity of $\sim 200\ \mu K\sqrt{s}$. The focal plane is arranged in a 4×4 grid with a spacing of $\sim 16'$ between beam centers on the sky.

The Viper telescope is a 2.1-m off-axis Gregorian telescope designed specifically for observations of CMB anisotropy. The primary is surrounded by a 0.5 m skirt to reflect illumination spillover to the sky. The entire telescope is enclosed in a large conical ground shield to block emission from elevations below $\sim 25°$; one section lowers to allow observations of low-elevation sources such as planets. A chopping flat at the image of the primary formed by the secondary sweeps the beams $\sim 3°$ in co-elevation in a fraction of a second.

The combination of large chop ($\sim 3°$) and small beam sizes ($\sim 4 - -5'$ FWHM Gaussians) makes ACBAR sensitive to a wide range of angular scales ($150 < \ell < 3000$), with high ℓ-space resolution ($\Delta\ell \sim 150$).

The Antarctic plateau provides an exceptional site to conduct millimeter-wave observations. The elevation at the South Pole is $\sim 9,300$ ft and the average ambient temperature during the austral winter is averages about $-80°$F. The high altitude, dry air, and lack of diurnal variation result in a transparent and extremely stable atmosphere (Lay & Halverson 2000, Peterson et al. 2002). Because of the low column depth of water, the average zenith opacity at 150 GHz (as measured with sky dips) is about 3%. The entire southern celestial hemisphere is available year-round allowing very deep integrations. When combined with a well established research infrastructure, these attributes makes the South Pole an ideal location for terrestrial CMB observations.

2. CMB Observations

The power spectrum reported in Kuo et al. (2002) is derived from observations of two separate fields, which we call CMB2 and CMB5. Data from two additional CMB fields taken during 2002 are currently being analyzed.

Each CMB field was selected to include a bright, unresolved, flat-spectrum radio source. The coadded image of this guide source is used to determine the effective beam sizes at the center of the map and includes smearing due to pointing jitter that occurs over the period in which the data are acquired. These final point-source image sizes are consistent with the beam sizes measured on planets and the observed pointing RMS determined from frequent observations of galactic sources.

3. Power Spectrum

We develop a *cleaned noise-weighted coadded map* as an intermediate step from time stream data to power spectrum. This technique identifies periods when the data have significant correlated atmospheric noise and adaptively projects out the corrupted spatial modes. After projection of the corrupted modes the data are weighted by their variance. The projection of modes and noise weighting are accounted for in the theory and noise covariance matrices.

The Lead-Main-Trail-differenced map of the CMB5 field is shown in Figure 1. The map pixelization is $2.5'$. For the purposes of presentation, we have smoothed the pixelized map with a $4.5'$ FWHM Gaussian. Due to differences in sky coverage, the noise varies across the map: in the central region, the RMS noise per $5'$ beam is found to be $17\,\mu$K and $8\,\mu$K for the CMB2 and CMB5 LMT-differenced maps, respectively. On degree angular scales, the S/N in the center of the CMB5 map approaches 100.

The maximum likelihood band powers are estimated iteratively using the quadratic iteration method of Bond et al. (1998). The ACBAR power spectrum – as well as the power spectra from other contemporary experiments – is shown in Figure 2. The decorrelated band powers and window functions are available on the ACBAR website[1].

4. Cosmological Parameter Extraction

Using Bayesian statistical techniques we combine ACBAR data with data from other CMB observations to derive estimates of cosmological parameters in inflation-motivated adiabatic CDM models. A complete treatment is presented in Goldstein et al. (2002). The addition of the ACBAR data to the previous body of CMB results has a substantial impact on the likelihood of models without a cosmological constant. The 3σ lower-limit is increased from $\Omega_\Lambda > 0.086$ for the "Other" CMB experiments to $\Omega_\Lambda > 0.136$ by including ACBAR. The χ^2 of best-fit free-Ω_Λ and $\Omega_\Lambda = 0$ models is $\chi^2 = 140$ and $\chi^2 = 160$ for 116 band powers, respectively. The hypothesis that the dark energy density is zero has become significantly unlikely.

Because of the high resolution of ACBAR, it is possible that sources of secondary anisotropy, such as from the Sunyaev-Zel'dovich effect in clusters that are not individually detected, could contribute significant power, exceeding the primary CMB spectrum at high-ℓ. However, the detection of power in the highest ℓ bin is only 0.9σ above the best-fit model CMB power spectrum. Thus, for cosmological parameter estimation based on the full ACBAR power spectrum we believe we can safely ignore the effects from the potential SZ contamination. As the precision of our high-ℓ data improves, however, we will have to include the SZ contribution in deriving parameter estimates.

[1] http://cosmology.berkeley.edu/group/swlh/acbar/

https://doi.org/10.1017/S0074180900196482 Published online by Cambridge University Press

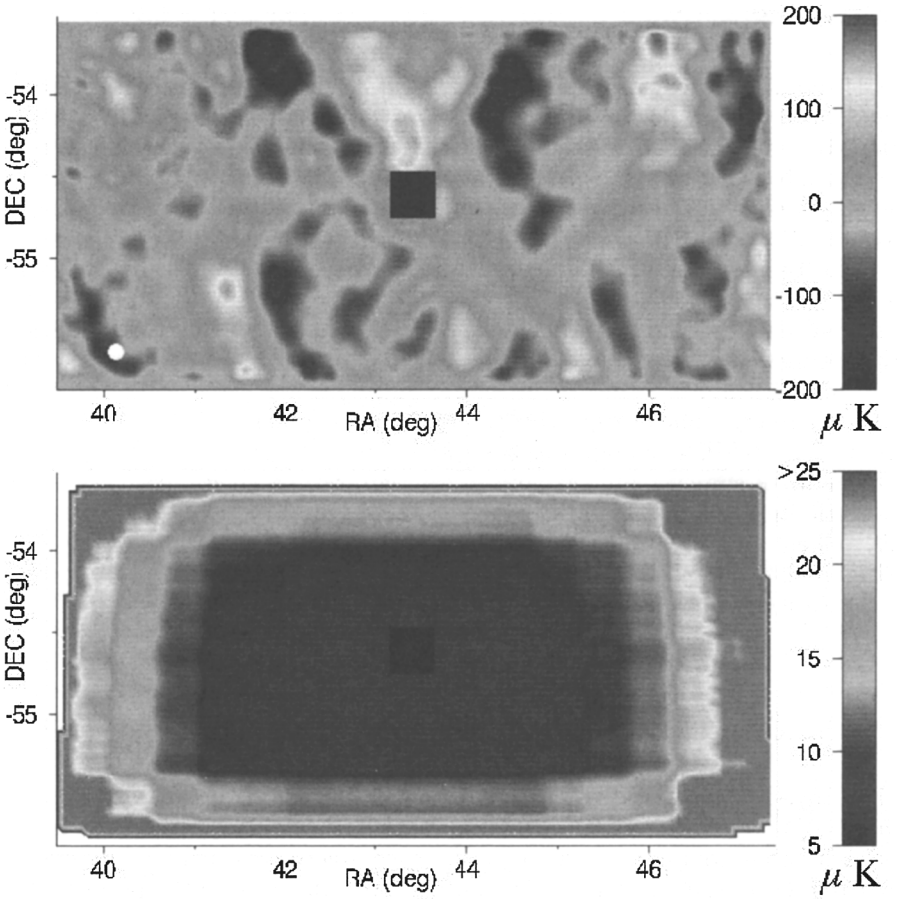

Figure 1. The top panel shows the LMT-differenced, atmospheric mode removed, noise weighted, coadded map for the CMB5 field. The guide quasar has been replaced with black pixels. The small white circle in the lower left hand corner of the map represents the FWHM of the average array element beam size as determined from the coadded quasar image. The map is pixelated at 2.5′ and has been smoothed with a 4.5′ FWHM Gaussian. The predominance of extended structure in the vertical direction results from deprojection of extended horizontal structure during atmospheric mode removal. The lower panel shows the noise in the LMT differenced map as a function of position. The S/N of the degree-scale structures in this map approaches 100. This figure is from Kuo et al. (2002).

5. Sunyaev-Zel'dovich Effect Observations

In addition to our measurement of the CMB anisotropy power spectrum, we are conducting the Viper Sunyaev-Zel'dovich Survey, a study of the SZ Effect in a complete sample of X-ray-bright galaxy clusters. During the 2001–2002 observing season we observed six clusters and present images of one, 1E0657−67 (z =0.299), here. This is one of the brightest X-ray clusters in the REFLEX

https://doi.org/10.1017/S0074180900196482 Published online by Cambridge University Press

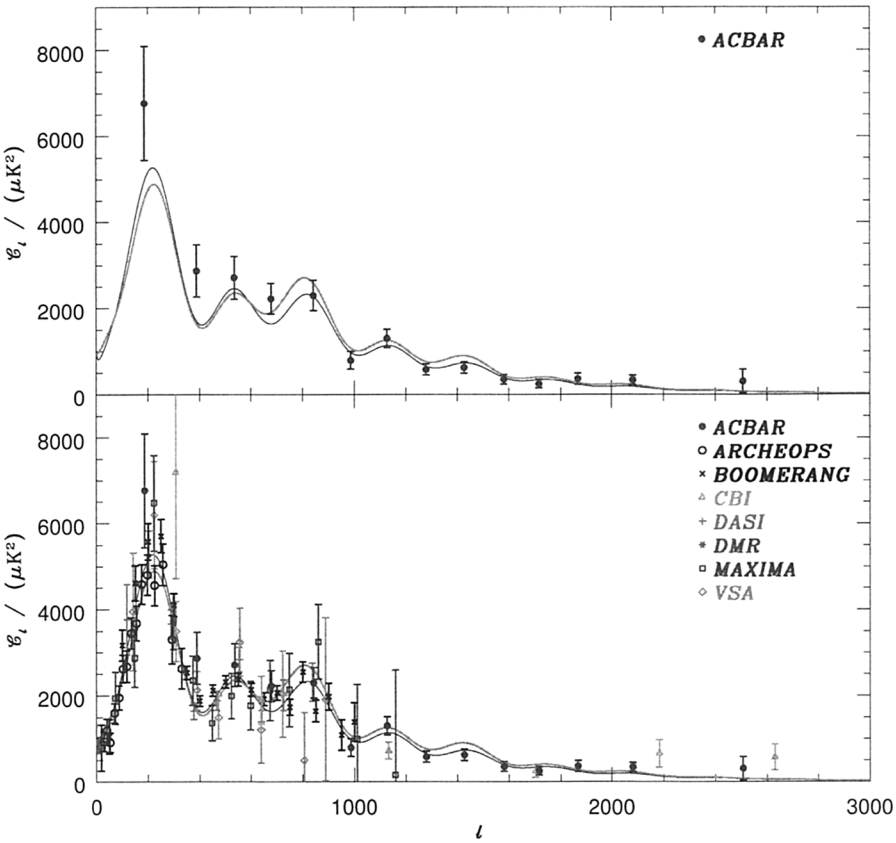

Figure 2. Top Panel: The ACBAR CMB power spectrum, $\mathcal{C}_\ell \equiv \ell(\ell+1)C_\ell/(2\pi)$, plotted over a vacuum energy dominated [$\Omega_k = -0.05$, $\Omega_\Lambda = 0.5$, $\omega_{cdm} = 0.12$, $\omega_b = 0.02$, $H_0 = 50$, $\tau_C = 0.025$, $n_s = 0.925$, amplitude $\mathcal{C}_{10} = 1.11\times10^{-10}T^2_{\rm CMB}$] model (thin line) and a CDM dominated [$\Omega_k = 0.05$, $\Omega_\Lambda = 0$, $\omega_{cdm} = 0.22$, $\omega_b = 0.02$, $H_0 = 50$, $\tau_C = 0$, $n_s = 0.925$, amplitude $\mathcal{C}_{10} = 1.34\times10^{-10}T^2_{\rm CMB}$] model (thick line). These are the best-fit models, for Λ and Λ-free models respectively, found during the ACBAR+Others parameter estimation described in Goldstein et al. (2002), with the weak-h prior. Bottom Panel: The top panel with the addition of power spectra from several other experiments. Both models appear to be reasonable fits to the data, with the $\Omega_\Lambda = 0.5$ model statistically being the better of the two. This figure is from Goldstein et al. (2002).

catalog that can be observed from the South Pole. We detected the thermal Sunyaev-Zeldovich effect from 1E0657−67 at 150 GHz and at 275 GHz (Figure 3). These are the first 2d-maps of the SZ effect on both sides of the thermal null. Moreover, we also report the non-detection at 220 GHz consistent with the expected null in the thermal SZ effect.

This cluster was first discovered using *Einstein* (Tucker et al. 1995). A ROSAT image confirmed the detection. Detailed *Chandra* X-ray and temperature maps derived by Markevitch et al. (2002) show that this cluster is the

https://doi.org/10.1017/S0074180900196482 Published online by Cambridge University Press

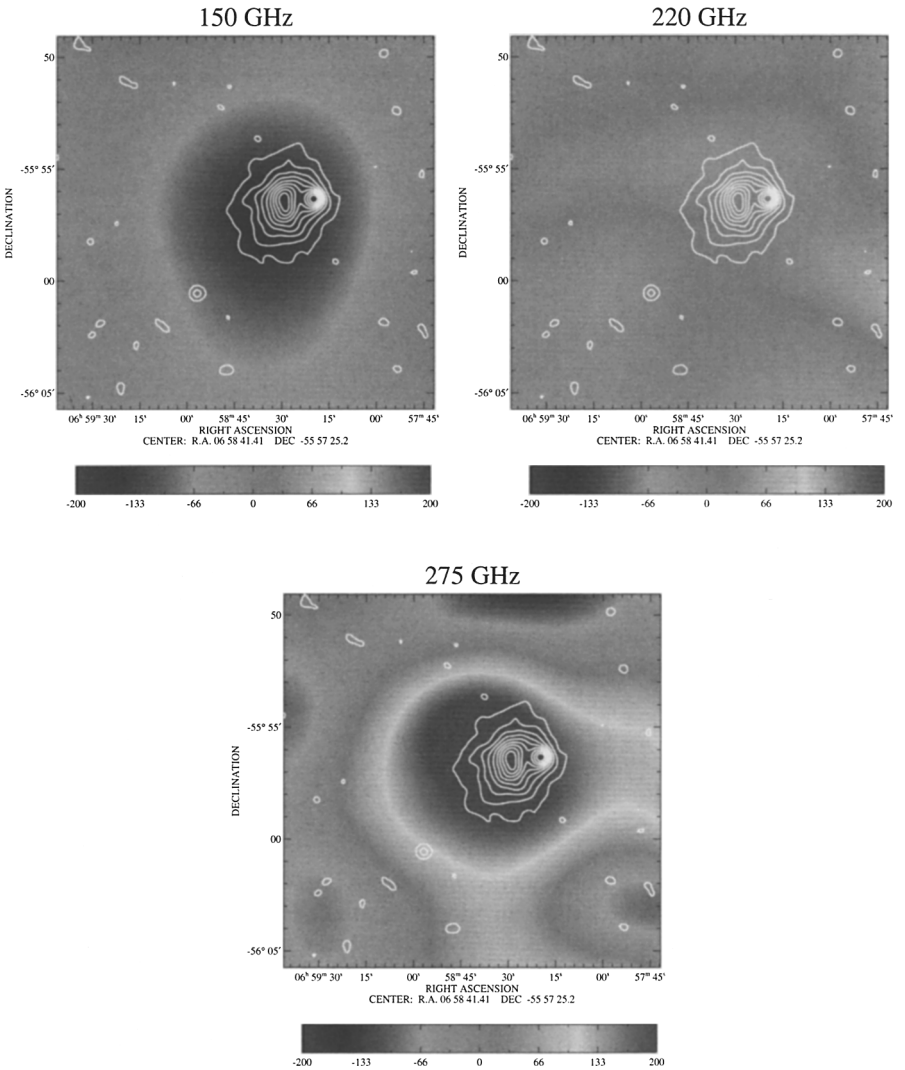

Figure 3. 150 GHz, 220 GHz, and 275 GHz ACBAR images of 1E0657−67 overlaid onto ROSAT HRI contours shown in white. The ACBAR beam size is $\sim$ 4.5 arcmin. The horizontal bar shows the CMB temperature scale of the maps in μK and ranges from -200 μK/beam to 200 μK/beam. The noise in each image is $\sim$ 10 μK/beam, 30 μK/beam, and 70 μK/beam respectively. The dimensions of each map are $\sim$ 15 arcmin $\times$ 15 arcmin.

product of a recent merger. The merger is so recent that the bulk shock produced by the core crossing is still strong (Mach number $\sim$ 2–3) and there is significant temperature substructure in the system. Temperatures range from 8 keV to more than 20 keV. Our observations revealed a peak SZ decrement of $\sim$ 180 μK/beam (with an error of 9 μK/beam), a peak increment of $\sim$ 180 μK (with an error of 66 μK/beam), and no detectable signal at 220 GHz. Note that

https://doi.org/10.1017/S0074180900196482 Published online by Cambridge University Press

our 150 GHz and 275 GHz detections confirm the SZ effect detection obtained by Andreani et al. (1999).

6. Discussion

The ACBAR experiment has been used to precisely measure the CMB sky from the South Pole and has produced the highest signal-to-noise map of the CMB to date. These data have yielded the most sensitive measurement of the damping tail region of the CMB power spectrum as of this writing. Analysis of the remainder of the 2001 through 2002 ACBAR data is underway and should further refine our power spectrum and parameter estimates. The data agree with the predictions of the flat-ΛCDM model with adiabatic initial perturbations. When considering the ACBAR data in combination with other contemporary CMB results, the addition of a single parameter, Ω_Λ, significantly improves the fit to the data.

After publication of the ACBAR results in late 2002, the WMAP team released their beautiful first-year CMB images, power spectrum, and cosmological parameter estimates (Hinshaw et al. 2003, Spergel et al. 2003). The beam size of the WMAP observations allows precise measurement of the power spectrum only below ($\ell \sim 800$) so the ACBAR and CBI data sets were used to "extend" the WMAP power spectrum (forming the WMAPext data set). The ACBAR damping tail data help break some of the degeneracies at low-ℓ, improving the precision of parameter estimates. In addition, the combined set provides marginal evidence for a "running" scalar index, $dn_s/d\ln k \neq 0$ (Spergel et al. 2003) that is bolstered by incorporation of galaxy redshift and Lyman-α survey results. The value of the scalar index and running index can be used to constrain inflationary models. Already CMB data have been used to claim that inflationary potentials of the form $V(\phi) \propto \phi^4$ are ruled out at the 3σ level (Kinney et al. 2003). More precise data in the damping tail region should assist in this endeavor. To this end we are working to improve the precision of the intercalibration of ACBAR, WMAP and Boomerang data.

Acknowledgments. The ACBAR program has been primarily supported by NSF office of polar programs grants OPP-8920223 and OPP-0091840. This research used resources of the National Energy Research Scientific Computing Center, which is supported by the Office of Science of the U.S. Department of Energy under Contract No. DE-AC03-76SF00098. Chao-Lin Kuo acknowledges support from a Dr. and Mrs. CY Soong fellowship and Marcus Runyan acknowledges support from a NASA Graduate Student Researchers Program fellowship. Chris Cantalupo, Matthew Newcomb and Jeff Peterson acknowledge partial financial support from NASA LTSA grant NAG5-7926.

References

Andreani, P., et al. 1999, ApJ, 513, 23
Bennett, C. L., et al. 1996, ApJ, 464, L1
Bond, J. R., Jaffe, A. H., & Knox, L. 1998, Phys.Rev.D, 57, 2117
Goldstein, J., et al. 2003, ApJ, 599, 773

Hinshaw, G., et al. 2003, ApJS, 148, 135.
Kinney, W. H., Kolb, E. W., Melchiorri, A., & Riotto, A. 2003, FERMILAB-Pub-03/117-A, hep-ph/0305130
Kuo, C. L., et al. 2004, ApJ, 600, 32
Lay, O. P., & Halverson, N. W. 2000, ApJ, 543, 787
Markevitch, M., et al. 2002, ApJ, 567, L27
Peterson, J. B., et al. 2003, PASP, 115, 383
Runyan, M. C., et al. 2003, ApJS, 149, 265
Spergel, D. N., et al. 2003, ApJS, 148, 175.
Tucker, W. H., Tananbaum, H., & Remillard, R. A. 1995, ApJ, 444, 532
Turner, A. D., et al. 2001, Appl.Optics, 40, 4921